Sports Eng (2010) 12:155–161
DOI 10.1007/s12283-010-0037-0

TECHNICAL NOTE

# Cycling shoe aerodynamics

**Giuseppe Gibertini · Donato Grassi · Carlo Macchi · Giuseppe De Bortoli**

Published online: 24 March 2010


**Abstract** The present paper describes the activity carried out to investigate the aerodynamic effects of cycling shoes for time trial competitions. This subject has not been widely studied but can be important for an accurate aerodynamic optimisation of a time trial cyclist. The study was carried out by means of wind tunnel testing: an appropriate test setup and an appropriate test procedure (based on "effective angle of attack approach") were developed in order to produce realistic test conditions. The developed testing procedure was applied to two different shoe models, differently fastened. Furthermore, an important point was the investigation of the overshoe effect. The results showed that the power required to overcome the shoe's drag is almost a tenth of the total power and that differences between the shoes can affect the cyclist's performance.

**Keywords** Cycling · Shoe · Wind tunnel

## 1 Introduction

Most of the athlete's power output in time trial cycling competitions is used to overcome aerodynamics resistance [1–3]. Thus, aerodynamic optimisation of the cyclist's position and equipment can improve the athlete's performance. An interesting but not so studied subject related to the cyclist's aerodynamics is that of drag due to the shoes, although more information can be found, for example, about the effect of helmet and body suit [4, 5]. The drag portion due to the body is clearly more important but any effect is attentionworthy in order to improve the cyclist's performance. The present paper reports a wind tunnel study carried out to evaluate the amount of drag (and therefore power loss) due to shoes when the athlete is pedalling and to compare the effects of two different shoes, namely a lace-up model and a strap fastened one. Furthermore, the effect of a tight overshoe (of the kind usually adopted by time trial racers) has been investigated. To achieve these aims an experimental procedure has been defined and the necessary instrumentation has been set up. The basic methodological guideline of this study was not the exact reproduction of the shoes operative conditions but the identification of a set of reference test conditions reasonably close to the real ones and easily reproducible with a good degree of repeatability. As a matter of fact the only way to be sure that the test conditions correspond to the real situation would be to resort to a complete manned configuration with a real athlete pedalling on the bicycle. But, on the other hand, in this case it would be really difficult to detect the specific shoes contribution and, furthermore, to obtain an acceptable degree of repeatability.

## 2 Definition of the problem

The motion of the shoe with respect to the ground is composed of the bicycle's horizontal advance and the motion of the shoe with respect to the bicycle due to pedalling. Considering nominal still air, the motion with respect to the ground is also the motion with respect to the air. In order to reproduce completely this varying

G. Gibertini (✉) · D. Grassi · C. Macchi
Dipartimento di Ingegneria Aerospaziale,
Politecnico di Milano, Via La Masa 34,
20156 Milan, Italy
e-mail: giuseppe.gibertini@polimi.it

G. De Bortoli
K22 Studio, Via Castellana 195,
31044 Montebelluna (TV), Italy

condition, one should reproduce in the wind tunnel the shoe motion around the bottom bracket axle. Nevertheless, at the relatively low speeds used, the reduced frequency values (see Sect. 4) are small enough that dynamic effects can be neglected and so the assumption of quasi-steady state is valid allowing steady condition tests to characterise the shoe aerodynamics. Of course the real conditions over the shoes change during each pedal rotation so that more tests have to be carried out for each shoe, covering a representative set of conditions. Four different conditions, identified by four different crankarm angle values $\theta$, have been taken as representative of the complete rotation and reproduced in the tests. The pitch angle $\varepsilon_F$ of the foot and the pitch angle $\varepsilon_S$ of the shank (see Fig. 1) in the four reference positions have been deduced from photograms of video recorded during a previous cyclist's wind tunnel test carried out in the Large Wind Tunnel of Politecnico di Milano (see Fig. 2). The angles, as deduced from the pictures, are listed in Table 1 together with the difference $\Delta\varepsilon = \varepsilon_S - \varepsilon_F$ representing the angle between the shank and the foot. Due to the low video resolution, the obtained values have to be taken as indicative and errors up to some degrees are possible but larger differences were found between different cyclists (compare Fig. 2 with Fig. 3). Thus, accurate determination of the real individual angles was not carried out, rather the representative values in Table 1 were obtained and kept constant.

## 3 The experimental setup and the tested models

The wind tunnel utilised for the present activity is a closed-loop facility with a test chamber 1 m wide, 1.5 m high and 2 m long. The test chamber turbulence level is of the order of 0.1% and the speed is controllable up to a maximum value of 55 m/s.

The test chamber dynamic pressure is determined from the measurement of the wall pressure difference between the inlet and the outlet of the contraction. This pressure difference is measured by a differential pressure transducer with 0.5 Pa accuracy.

The test layout included the presence of the parts that are expected to produce the largest interferences with the shoe: the shank and the pedal (without the crankarm). Thus the pedal effect is included in the measurements and is not possible to separate from the shoe effect while the crank effect is not reproduced. This means, of course, that the present setup is a simplified model of the actual situation and not all the possible interference effects are reproduced in the tests. Nevertheless, the most important effects are included in the adopted layout.

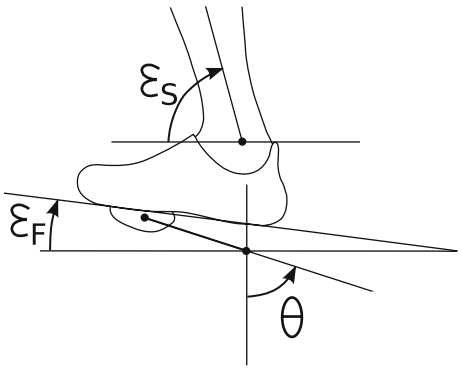


**Fig. 1** Definition of pedal/foot angles

**Fig. 2** Photogram of pedalling phase $\theta = 0$

**Table 1** Pitch angle (in radians) measured from the pictures

| $\theta$ | $\varepsilon_F$ | $\varepsilon_S$ | $\Delta\varepsilon$ |
|---|---|---|---|
| 0 | −0.40 | 0.86 | 1.26 |
| $\pi/2$ | 0.15 | 1.41 | 1.26 |
| $\pi$ | −0.29 | 1.46 | 1.75 |
| $3\pi/2$ | −0.71 | 0.71 | 1.42 |

**Fig. 3** A different biker at the same pedalling phase

The shoes with the pedal have been mounted on a foot shape hinged to a beam with the top extremity shaped as a shank. The lower extremity of the beam was hinged to a mechanical interface fixed over a six-component wind tunnel balance. The balance precision is in the order of 0.01 N for all the force components. This strut allowed for different angular setting of both foot and shank as sketched in Fig. 4. During the test activity the beam inclination with respect to the test chamber was set using a clinometer, while the different foot inclinations over the beam were fixed by apposite holes and pins. The uncertainty of both these two settings was in the order of a tenth of degree. A global view of the experimental setup is shown in Fig. 5.

Three different shoe models (all with European size 42) were tested:

- shoe A, laced up and with a very "clean" and close-fitting shape (Fig. 6a)
- shoe B, strap fastened (Fig. 6b).

The pedal is a clipless single-sided model, extending 33 mm below the sole. Further tests were carried out covering shoe B with an overshoe (see Fig. 7).

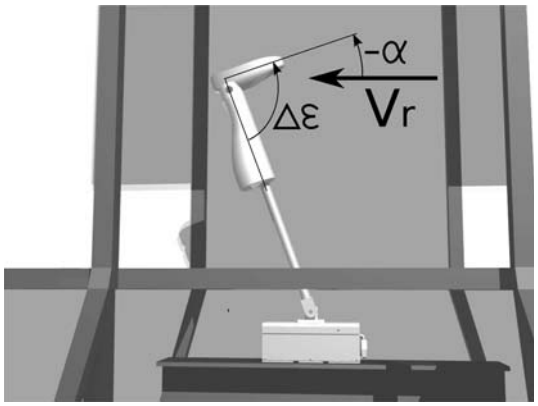


**Fig. 4** Sketch of the experimental setup with reference direction definition

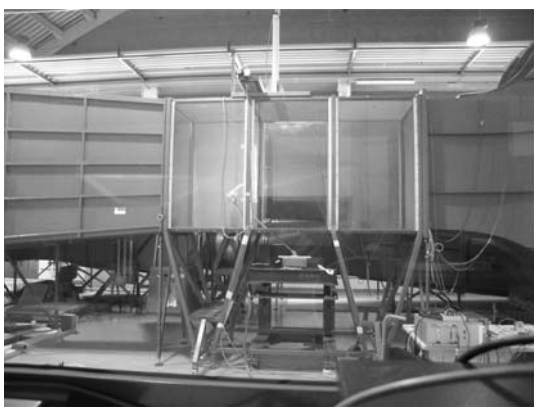

**Fig. 5** A view of the experimental setup

Furthermore, tests of Shoe B with and without the overshoe have been repeated with a quite different pedal model to verify that the obtained results did not depend on the particular pedal model used.

## 4 Test procedure

As mentioned in Sect. 2 the air velocity $\mathbf{V}_r$ relative to the foot is due to the bicycle advancing and to the pedalling. Furthermore, the motion of the foot due to pedalling can be resolved into a translational motion around the crankarm bottom axle and a rotation due to the foot pitching. The first effect is simply accounted for by means of a vector sum with the bicycle translation, while the dynamic effect of the foot pitch oscillation is neglected (corresponding to the use of an "effective angle of attack approach" [6]) as the reduced frequency $k$ is rather small. For an airfoil of chord $c$, unsteadiness effects start to be important for $k > 2\pi fc/(2V) > 0.5$ (see [7]) while in the present case, considering the pedalling frequency $f = 1.8$ Hz and taking a chord $c$ equal to the shoe length, a value of $k$ in the order of 0.1 is obtained.

Finally, defining the vector $\mathbf{V}_r$ by means of its absolute value $V_r$ and its incidence angle $\alpha$ respect to the foot, it is possible to write the following relations:

$$V_r = \sqrt{(V_B + \dot{\theta} a \cos\theta)^2 + (\dot{\theta} a \sin\theta)^2} \tag{1}$$

$$\alpha = \varepsilon_F + \arctan\left(\frac{\dot{\theta} a \sin\theta}{V_B + \dot{\theta}\, a \cos\theta}\right) \tag{2}$$

where $a$ is the length of the crankarm that is assumed to be 0.175 m.

To determine the experimental conditions a bicycle velocity $V_B = 15$ m/s $= 54$ km/h and a pedalling frequency $f_P = 1.8$ Hz, corresponding to an angular velocity $\dot{\theta}_S = 11.3\,\mathrm{rad/s}$ have been assumed. The four test conditions, according to Eqs. 1 and 2, are listed in Table 2 where the nominal dynamic pressure $q_r$ has been calculated as $q_r = \frac{1}{2}\rho_{st} {V_B}^2$ where $\rho_{\mathrm{st}} = 1.225\ \mathrm{kg/m^3}$ is the standard air density. It is noteworthy that the aerodynamic incidence angle $\alpha$ is negative at three pedalling phases among the four ones considered.

For each test condition (corresponding to a certain value of the crankarm angle $\theta$), the foot inclination inside the wind tunnel test section was set equal to the corresponding incidence angle according to Table 2 and the shank inclination was set, with respect to the foot, at the corresponding angle $\Delta\varepsilon$ according to Table 1.

The acquisition of balance signals before each test provides the effects of weight and zero drift to be eliminated. Furthermore, in order to be able to obtain the net

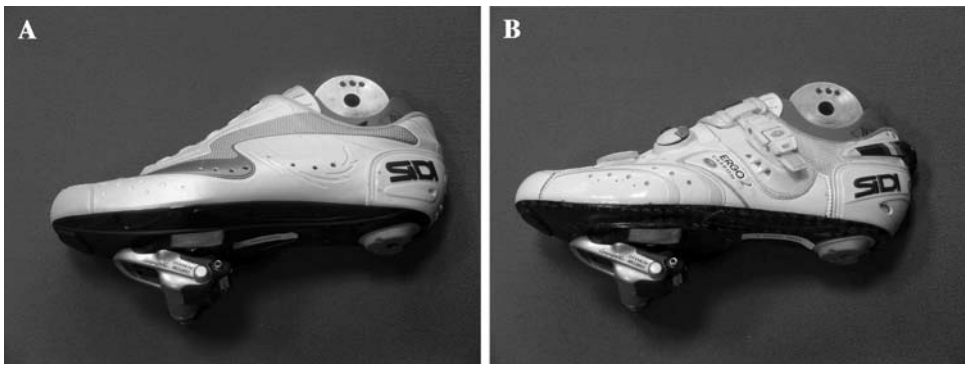


**Fig. 6** The shoe models

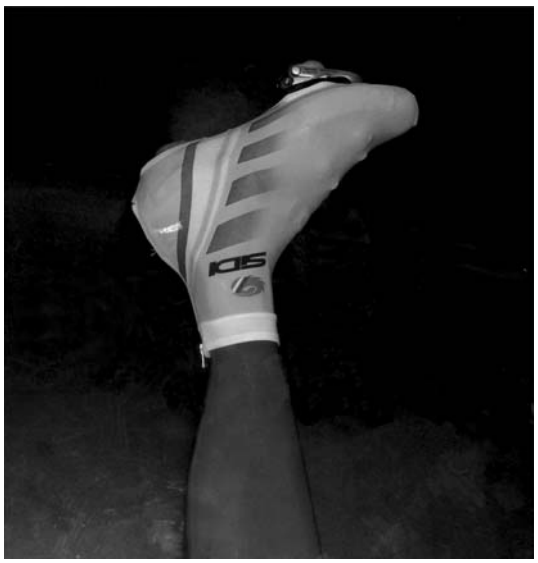

**Fig. 7** The overshoe

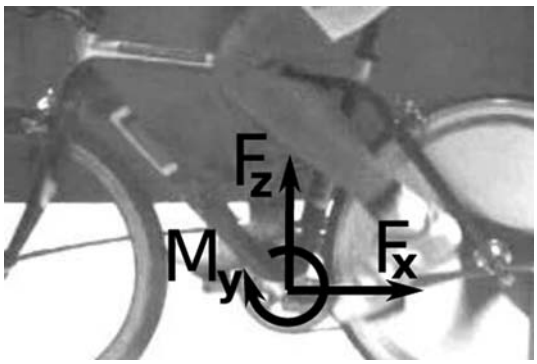


**Fig. 8** Force and moment reduced to the bottom bracket axle

**Table 2** Test conditions

| $\theta$ (rad) | $V_r$ (m/s) | $q_r$ (Pa) | $\alpha$ (rad) | $\alpha$ (°) |
|---|---|---|---|---|
| 0 | 17.0 | 177 | −0.40 | −23 |
| $\pi/2$ | 15.1 | 140 | 0.28 | 16 |
| $\pi$ | 13.0 | 104 | −0.29 | −17 |
| $3\pi/2$ | 15.1 | 140 | −0.84 | −48 |

aerodynamic loads acting on shoe and pedal, previous foot-off tests (with just the beam and the shank) have been carried out to measure the aerodynamic tares [8].

For each test, forces and moments were obtained as the mean values of the data acquired for a period of 30 s at a frequency of 1 kHz.

## 5 Results and discussion

The tests were carried out under ambient atmospheric conditions but the atmospheric air density is not constant and is generally different from the standard value $\rho_{st}$. Furthermore, the wind tunnel control keeps the required speed inside a tolerance interval of ±0.5 m/s. Thus, in order to ensure a better comparability of the results, the measured loads were reduced to the nominal conditions by multiplying them by the ratio between the nominal dynamic pressure $q_r$ and the actual wind tunnel dynamic pressure. Furthermore, the measured loads were reduced to a force **F** and a moment **M** acting on the bottom bracket axle. An $xyz$ reference system has been adopted where the $x$ axis is horizontal and backward while the $z$ axis is vertical and upward (and therefore the $y$ axis is parallel to the crankarm axle and directed to the right of the cyclist). This reference system has been used to project the force and moment components as shown in Fig. 8.

The system was not visibly oscillating and the force amplitude spectra did not show excessive unsteadiness. For example, the amplitude spectrum of the measured gross force $F_x$, including the action on the strut and the shank, presented in Fig. 9 shows that the harmonic amplitudes normalised with respect to the mean value are rather small.

Eight tests have been carried out for each condition founding a measurement repeatability (three times the standard deviation) smaller than 0.04 N for both $F_x$ and $F_z$.

The results obtained for the three different shoe configurations at the four different crankarm angles are listed in Table 3. The force measured values are of the same

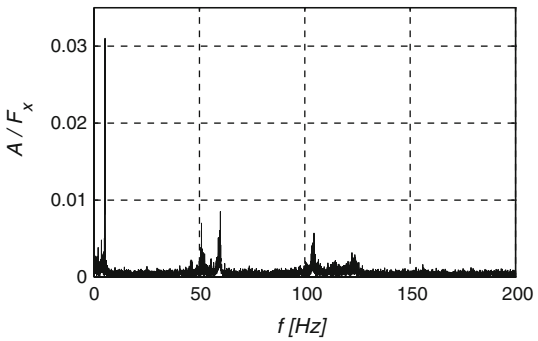


**Fig. 9** $F_x$ amplitude spectrum

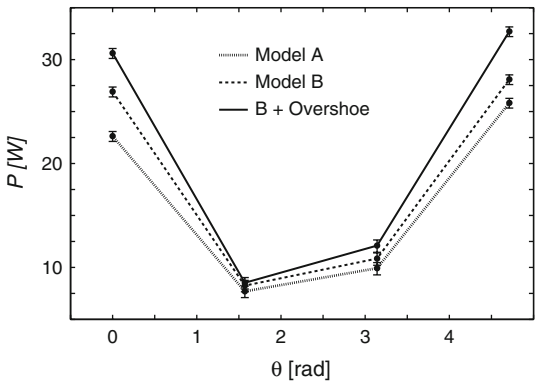


**Fig. 10** Power requirement by the three different shoes at the four crankarm angles

order of magnitude as the value obtained by Asai et al. [9] for a running shoe tested in a wind tunnel at 15 m/s although the shoe model and the test layout were different. As a matter of fact, the work of Asai et al. is quite different from the present one: first of all for the different kind of shoe, but much more for the different test conditions because in that case no shank model was present and the shoe alone was held over the wind tunnel pylon in such a way that the incoming flow could blow directly inside the shoe. Due to these differences a direct comparison between the two studies is not possible but, due to the lack of other publications about the subject of shoes aerodynamics, the fact that the measured forces are not so different is supporting evidence for the results of this study.

The power required to overcome the aerodynamic effects over the shoe can be calculated using the following equation:

$$P = F_x V_B + M_y \dot{\theta} \tag{3}$$

Figure 10 shows the power required for the three different shoes (with the uncertainty bars). This shows that the best results are obtained with the laced close-fitting "model A" while the worst result (the highest absorbed power) was obtained with the overshoe. It can be observed that the shoes are essentially bluff bodies so that their drag is mainly due to the pressure distribution and is strongly related to the projected frontal area. In Fig. 11 the front view of shoes A and B are presented: the projected frontal area at zero incidence is $94 \times 10^{-4}$ m$^2$ for the shoe A and $96 \times 10^{-4}$ m$^2$ for the shoe B. The difference in frontal area between the shoes is insufficient to explain the differences in drag and $P$ (Fig. 10). The buckles for shoe B, Fig. 11, represent a bluff body and so would increase drag. The effect of the buckles and the steps associated with the straps would account for the increased drag shown by shoe B in comparison with shoe A. The use of an overshoe should smooth out the buckles and straps (Fig. 12) leading to a reduction in drag, but this is accompanied by an increase in frontal area, which gives a greater increase in drag so that the net effect is an overall increase in drag and power requirement. The overshoe encompasses the ankle too and the increase in the frontal area with respect to uncovered shoe and ankle is $6.4 \times 10^{-4}$ m$^2$.

It is interesting to note that the power requirement is higher when the incidence is negative, i.e. when the flow has a component directed from the instep to the sole (possible solutions to improve the aerodynamic efficiency of the shoes should take this into account). It is also observable that for $\theta = \pi/2$ (where the incidence is positive and the power is minimum) the three shoe configurations produced quite close values of the power required. This closeness is probably due to the fact that in this case, as the flow comes from below, the interaction is dominated by the shape of the sole (with the pedal) that is essentially the same for all three configurations (the pedal is exactly the same).

**Table 3** Measured aerodynamic loads

| $\theta$ (rad) | Model A | | | Model B | | | B + Overshoe | | |
|---|---|---|---|---|---|---|---|---|---|
| | $F_x$ (N) | $F_z$ (N) | $M_y$ (Nm) | $F_x$ (N) | $F_z$ (N) | $M_y$ (Nm) | $F_x$ (N) | $F_z$ (N) | $M_y$ (Nm) |
| 0 | 1.28 | −0.56 | 0.299 | 1.50 | −0.67 | 0.389 | 1.69 | −0.89 | 0.466 |
| $\pi/2$ | 0.60 | −0.45 | −0.107 | 0.64 | −0.48 | −0.123 | 0.66 | −0.55 | −0.119 |
| $\pi$ | 0.72 | −0.37 | −0.114 | 0.80 | −0.35 | −0.098 | 0.92 | −0.49 | −0.147 |
| $3\pi/2$ | 1.37 | −0.11 | 0.435 | 1.54 | −0.44 | 0.435 | 1.78 | −0.43 | 0.532 |

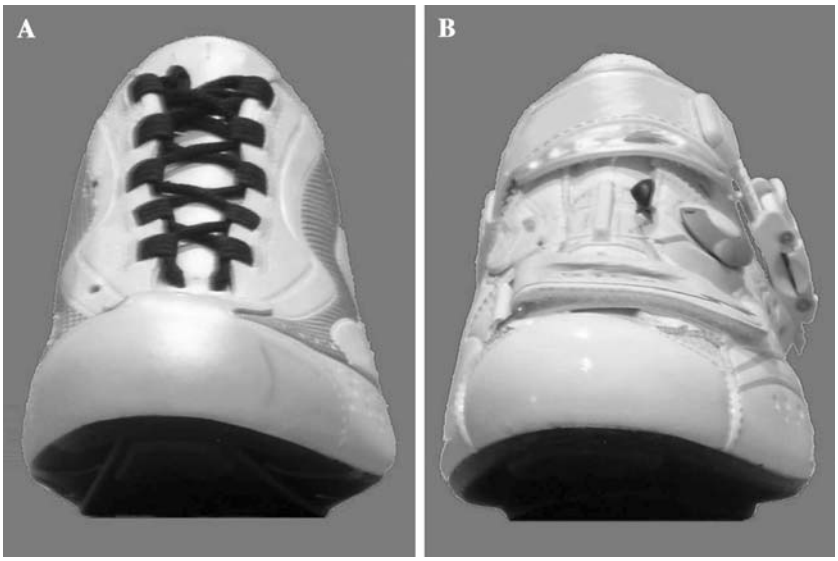


**Fig. 11** Front view of the shoes

**Fig. 12** Front view of the overshoe

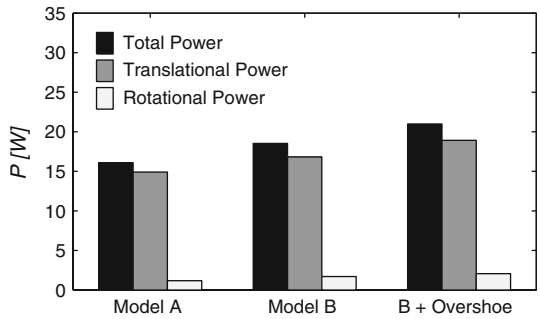


**Fig. 13** Comparison between the mean values of power request

A comparison between the average values (the arithmetic mean of the four values related to the four crankarm angles) is presented in Fig. 13. The figure also shows a decomposition of the total power into translational (due to force and bicycle translation) and rotational (due to torque and rotation around the bottom bracket axle) components.

The power associated with a single shoe was of the order of 20 W while the aerodynamic power required by a cyclist at this velocity can be roughly estimated as 500 W. This means that the power request to overcome the aerodynamic action over the two shoes is approximately 8% of the power required to overcome total air resistance. But the most important result is constituted by the non-negligible differences between the three different shoe configurations. The use of the overshoe, for example, increases the power needed by 2.5 W for each foot which means an increase in the order of 1% of the total power. This power gain is not negligible: as an example, a simple estimation in the case of a 10 km time trial competition leads to a gain of 2 s.

## 6 Conclusion

A test procedure has been developed that isolates the shoe aerodynamic problem allowing for affordable tests with reasonably realistic conditions. The results showed that the amount of power associated with the aerodynamic resistance of the shoes is a non-negligible part of the total power and that a proper choice of the shoe can produce a power gain. The best choice was shown to be a very simple laced

shoe closely fitting the cyclist's foot. On the contrary the use of the overshoe produces a noticeable disadvantage. The obtained results can be useful in further improvement of cycling aerodynamics efficiency and can lead to the development of possible solutions to reduce the power required to overcome the shoe resistance. Finally, it has to be outlined that the present study is an initial study into this area and further systematic investigations are needed to fully explain this phenomenon.

## References


1. Lukes RA, Chin SB, Haake SJ (2005) The understanding and development of cycling aerodynamics. Sports Eng 8:59–74
2. Gibertini G, Grassi D (2008) Cycling aerodynamics, in sport aerodynamics. CISM Courses and Lectures, Springer, Wien, 506:23–47
3. Oggiano L, Leirdal S, Sætran L, Ettema G (2008) Aerodynamic optimization and energy saving of cycling postures for international elite level cyclists. In: The engineering of sport 7. Springer, Paris, 1:597–604
4. Blair KB, Sidelko S (2008) Aerodynamic performances of time trial helmets. In: The engineering of sport 7. Springer, Paris, 1:371–377
5. Brownlie LW, Gartshore I, Chapman A, Banister EW (1991) The aerodynamics of cycling apparel. Cycl Sci 3:3–4
6. McGowan GZ, Gopalarathnam A, Ol MV, Edwards JR (2009) Analytical computational and experimental investigations of equivalence between pitch and plunge motions for airfoils at low Reynolds numbers, AIAA 2009-535, pp 17
7. Brunton SL, Rowley CW, Taira K, Colonius T, Collins J, Williams DR (2008) Unsteady aerodynamic forces on small-scale wings: experiments, simulations and models, AIAA 2008–520, pp 12
8. Barlow JB, Rae WH, Pope A (1999) Low-speed wind tunnel testing. Wiley and Sons, New York
9. Asai T, Seo K, Oda T, Orei T (2005) A study on aerodynamics of athletic spike shoes. In: 7th symposium on footwear biomechanics, Cleveland, Ohio, pp 82–83